Cutting the Cord: Soft Haptic Devices without a Pressure Source

Nathan Usevitch[1,2] and Andrew Stanley[1]

***Abstract*— We present a class of pneumatic haptic devices that use the input motion from a user to pump fluid in a closed pneumatic circuit, meaning that the pneumatic devices require no external pressure supply. The user is coupled to a pneumatic actuator in one direction such that user motion drives fluid from the coupling device to an accumulator. When released, fluid passively returns to the user coupling until a pressure equilibrium is reached. The stiffness felt by the user is changed by opening and closing a valve between the user coupling and the accumulator. We present and experimentally validate models that characterize the system in terms of the impedance felt by the user and the speed at which the coupling refills after it has been compressed, which gives a measure of the bandwidth of the system. We give two demonstrations: one where we modulate the resistance to finger bending, and another where we enable a small actuator worn on the fingertip to create button-like haptic sensations when pressed on a flat surface.**

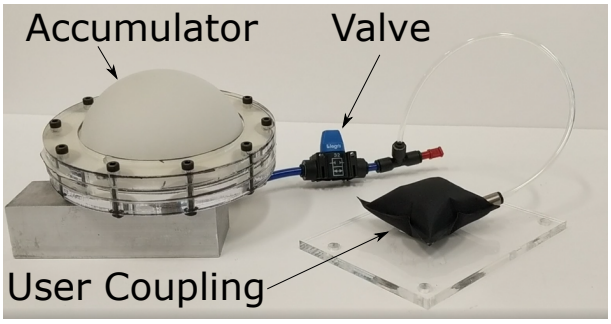

Fig. 1. An overview of the system that features a capacitor, a valve, and a user coupling device. No pressure supply is needed. The effective stiffness of the end effector can be switched between high and low by opening or closing the valve.

I. Introduction

Soft robotics systems are strong candidates for use in wearable haptic devices. The inherent compliance of soft actuators allow them to interface well with the human body and provide inherent safety. Pneumatic soft actuators can be designed to exert large forces and can change dramatically in size from their unactuated to actuated state, allowing them to have low encumbrance when not actuated. Often soft pneumatic actuators are composed of materials that are already used in wearable device design, such as fabrics. A key drawback of pneumatic soft robotic systems is that many depend on a rigid, externally mounted pump or air supply as a pressure source.

In this paper we present a soft robotic device that uses the energy of human input to pump fluid throughout a closed circuit. By tuning the passive characteristics of the pneumatic circuit, different sensations can be rendered to the user. In this work, we perform this tuning by making the binary decision to open and close a valve. A representative system is shown in Fig. 1, and consists of a fabric actuator that we call a "user coupling," a circuit with a valve, and a container that we refer to as an "accumulator." We characterize the resulting system in terms of dynamic range (the change in impedance felt by the user when the valve opens and closes), and the bandwidth, which corresponds to the flow rate between the user coupling and the accumulator. The pneumatic device opposes human motion and cannot apply any active forces. While limiting in some regards, it also guarantees the passivity of the device for haptic applications.

[1]Facebook Reality Labs, Redmond, WA , USA
[2]Stanford University Department of Mechanical Engineering
Contact usevitch@stanford.edu, andrew.stanley@oculus.com

Our approach is most similar to the approach in [1], where opening and closing of a valve to impede or allow flow through a fluidic flexible matrix composite was used to control stiffness. Our work uses a compressible fluid and applies similar ideas directly to an application in haptics.

The desire to develop untethered pneumatically actuated soft robots has drawn extensive research, with some of that work reviewed in [2]. In [3] a chemical reaction in a completely soft robot provides the air pressure. In [4] a soft robot is strong enough to carry an onboard compressor, and in [5] an onboard compressor powers slow motion while an explosive actuator enables jumping. Using explosives or combustion to provide pressure is not readily amenable to haptic applications, and other onboard pressure methods tend to be relatively slow. For haptic applications, speed and magnitude of force are critical, which leads us to propose a system where human input force provides the energy to the pneumatic circuit.

Passive devices to generate forces that resist human motion have been well explored in haptics. We refer to these devices as endogenous, where the device only resists human motion, as opposed to exogenous, where the device adds energy to the system. Many examples of endogenous haptic systems use either jamming or braking devices. In [6] particle jamming is used as a shape changing device, while in [7] particle jamming is used as an endogenous device, and a single exogenous pressure input is used. In [8], [9] layer jamming is used to resist motion. In [10] a mechanical brake is used on a rigid, holdable device to simulate grasping objects. We note that in general, these components primarily resist motion but provide no restoring force once they slip. If the device is pushed past the locking point, the new locking point is different. Our device is different in that the force applied not

only resists motion but also provides a restoring force, acting more as a spring than as a brake.

This paper is organized as follows: in Sec. II we discuss the design of the system, and in Sec. III and IV we discuss our modeling of the impedance and bandwidth of the system. In Sec. V we discuss experiments to validate these models, and in Sec. VI we discuss using the model to inform system design. In Sec. VII we demonstrate devices that resist bending of the finger and provide haptic feedback when pressing a virtual button on a flat surface.

II. System Overview

Our proposed device architecture is a closed pneumatic system that consists of the user coupling device, a fluid storage device that we call the accumulator, and a transmission between the two that contains a controllable electromechanical valve. The user coupling could be any existing pneumatic actuator. Motion of the user increases pressure in the coupling and drives fluid into the accumulator. When the user moves in the opposite direction, pressure in the coupling drops and fluid flows from the accumulator back into the coupling. We note that in many cases of haptic interaction one sided coupling is desired. For example simulating an object within the hand requires blocking the fingers from moving inward, but allowing them to move outward with little impedance. For our experiments, we choose the user coupling to be a device composed of flexible but inextensible materials, in this case ripstop nylon fabric coated in thermoplastic polyurethane (TPU). Devices composed of flexible but inextensible materials are well suited for one sided coupling because if the user moves such as to cause vacuum in the device, they collapse to near 0 volume and apply minimal force to the user.

In modeling this system, we will make use of an electrical analogy. In schematic form, we can think of the system as the two circuits shown in Fig. 2, where pressure is analogous to voltage, and current analogous to mass flow rate. When the user's motion is driving fluid into the accumulator, the coupling serves as a pressure source as shown in Fig. 2a, causing mass to flow through the circuit and be stored in the accumulator, which is analogous to a capacitor. When the human motion is not driving fluid through the circuit, both the accumulator and coupling function as capacitors and fluid passively flows from the accumulator to the user coupling as shown in Fig. 2b.

We choose air as the working fluid in our pneumatic circuit. While using an incompressible working fluid would allow for higher maximum stiffness, it would also increase the resistance to flow through the valve, sacrificing the low impedance state and leading to slower dynamics. In addition, an incompressible fluid requires that the accumulator be flexible, which adds some level of complexity to the mechanical design. If the circuit uses a compressible fluid, any volume can serve as an accumulator. While we have experimented with flexible accumulators such as the one shown in Fig. II, we will use only rigid accumulators in our experiments.

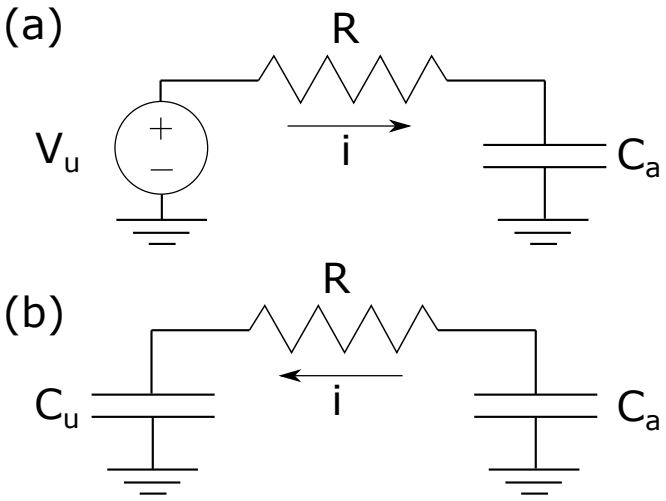

Fig. 2. Electrical analogies of the fluidic circuit. Diagram (a) corresponds to the case when the user is driving fluid out of the coupling and into the accumulator. Note that if the user motion is slow, the flow rate is small and the effect of the resistance is relativity small. In (b) both the coupling and the accumulator act as capacitors. Initially $P_u < P_a$ and after some transition, equilibrium is reached when the $P_u = P_a$. The behavior of the fabric pouch as a capacitor is discussed in Sec. IV.

III. Impedance Modeling

In this section we present a model that describes the impedance of the device and how it changes with different user couplings and accumulators. We denote the pressure and volume of the user coupling as P_u and V_u, and the pressure and volume of the accumulator as P_a and V_a. We assume that the temperature of the fluid is constant, and because the system is closed, we note by conservation of mass and the ideal gas law that $P_uV_u + P_aV_a = P_0(V_{u0} + V_{a0})$, where P_0 is the initial pressure of the entire system at equilibrium, and V_{u0} and V_{a0} are the initial volumes of the user coupling and the accumulator.

When the user is moving slowly, we note that $P_u \approx P_a$, and the impedance felt by the user does not depend on the dynamics of the circuit. When moving at higher frequency, the dynamics of the fluidic circuit in Fig. 2a will influence the impedance felt by the user. We will first present a model for the quasistatic impedance and then discuss the effect of the circuit dynamics when moving at a faster rate.

A. Quasistatic Impedance

In this section we develop a relationship between how much the user coupling is compressed and the resultant force and pressure of the system. In all of our experiments, the coupling is fabricated from materials that are flexible, but not stretchable, in our case TPU backed fabrics. In modeling the system we note that as long as the pressure inside the fabric pouch is higher than atmospheric pressure ($P_u > P_{atm}$), the shape of the actuator is approximately constant. This means that we can express $V_u = f(x)$, where x is a generalized displacement of the volume. If the user coupling were made of some other flexible material, we could write $V_u = f(P_u, x)$. In our initial derivation of the model, we will assume $V_u =$

$f(x)$ and that V_a is constant (meaning that the capacitor is a rigid container).

We develop our model using the principle of virtual work to relate the force applied to the user and the resultant displacement to the work done by the fluid

$$(P - P_{atm})dV = -F dx. \tag{1}$$

As the system is closed, by Boyle's law we can write

$$P(x) = \frac{P_0 V_0}{V(x)} \tag{2}$$

$$F = -\left(\frac{P_0 V_0}{V} - P_{atm}\right)\frac{dV}{dx}. \tag{3}$$

We now take the derivative with respect to position to obtain the stiffness, K:

$$K = \frac{dF}{dx} = P_0 V_0 \left(\frac{\frac{dV}{dx}}{V}\right)^2 - \left(\frac{P_0 V_0}{V} - P_{atm}\right)\frac{d^2V}{dx^2}. \tag{4}$$

Our goal is to understand what change in stiffness is achieved by shutting the valve between the user coupling and the accumulator. With the valve open and assuming a quasistatic condition, $V = V_0 = V_a + V_u$. When the valve closes, we define a new value for V and V_0 such that $V = V_0 = V_u$. Assuming a rigid accumulator, $\frac{dV}{dx}$ and $\frac{d^2V}{dx^2}$ are unchanged by closing the valve. If we assume $\frac{d^2V}{dx^2} = 0$, as is the case of a rigid piston actuator, we obtain the following as the ratio of stiffnesses when the valve is open and closed, thus characterizing the dynamic range of the device:

$$\frac{K_{closed}}{K_{open}} = \frac{V_u + V_a}{V_u}. \tag{5}$$

This indicates that for a rigid accumulator, increasing the stiffness by a factor x requires the ratio of the closed and open volume to be x. So for a 10x stiffness change, the ratio of closed to open volumes must be 10. While large, instantaneous changes in stiffness require large ratios of volumes, we note that force and stiffness, in (3) and (4), continue to increase rapidly with displacement. This indicates that while at modest ratios of volumes only modest instantaneous changes in stiffness can be obtained, the device can still exert large forces. We also note that a larger ratio of stiffness is possible if a flexible accumulator is used, as the terms $\frac{dV}{dx}$ and $\frac{d^2V}{dx^2}$ are changed by closing the valve and removing the compliance of the accumulator from the system.

IV. Bandwidth

When the user stops compressing the actuator, the user coupling must be able to quickly and passively refill with air. To analyze this process, we must compute the response time of the dynamic circuit shown in Fig. 2b. We choose to represent the resistance of the entire circuit between coupling and accumulator, including the tube, valve, and other features, as a single resistance element using the following approximate relationship for a compressible fluid given in Rennels et al [11],

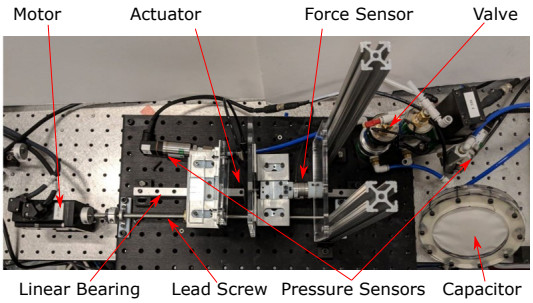

Fig. 3. The test setup. The fabric user coupling is placed between two parallel plates whose position is controlled by a servo motor. Pressures in coupling and accumulator are measured, as is the output force.

$$P_a - P_u = C\frac{\dot{m}^2}{\rho_u A^2} \tag{6}$$

where $\dot{m}$ is the mass flow rate of the fluid, A the orifice area and C is an engineering parameter. As we use this relationship to account for all of the resistance of the system including that of the valve, the tubing, and other components, we will experimentally fit a value of $\frac{C}{A^2}$. We denote the mass in the user coupling and the accumulator as m_u and m_a respectively, and by conservation of mass and the ideal gas law write $m_a = \frac{P_0(V_u+V_a)}{RT} - m_u$, where P_0 is the equilibrium pressure of the circuit. From the ideal gas law, $P_a = \frac{m_a RT}{V_a}$. The relationship of mass to pressure is more involved for the fabric user coupling. If the fabric pouch is flattened, air that enters the coupling causes it to expand at constant pressure P_{atm}. Once the fabric pouch has expanded to its final volume it then acts as a rigid container. Mathematically we express this relationship as

$$P_u = \begin{cases} P_{atm} & m_u < \frac{P_{atm}V_{u,max}}{RT} \\ \frac{m_u RT}{V_u} & m_u \geq \frac{P_{atm}V_{u,max}}{RT}. \end{cases} \tag{7}$$

We formulate a first order nonlinear ordinary differential equation where the state is the mass of air in the user coupling (m_a) by combining the resistance relationship in (6), with the pressure and mass relationships for the accumulator and the coupling. In the experimental section we solve this equation numerically and compare our experimental results with this model.

V. Experimental Results

A. Test Setup

We developed a test setup to evaluate the performance of the proposed devices as well as the validity of the models for impedance and response time presented in Sec III. The experimental setup is shown in Fig. 3. In the setup, we place a fabric user coupling device between parallel acrylic plates. These plates are mounted on a linear bearing and provide the squeezing force. The position of one of the plates is controlled by a lead screw driven by a servo motor with closed loop position control. We measure the forces applied

by the device using an ATI Nano 25, which is mounted behind the stationary acrylic plate. The setup runs the control on a desktop computer, with control and sensors managed through a NI Daq RIO. In our experiments, our user coupling device is created by sealing the edges of two flat squares of fabric. We attach a threaded push-to-connect coupling through the side with an o-ring around the threads. We measure the pressure by inserting a "T" joint with a pressure sensor as close as possible to where the tube exits the fabric coupling and accumulator.

B. Impedance

We wish to relate the motion of the device to the pressure (as predicted in (2)) and force (as predicted in (3)). In order to apply the model, the relationship between the displacement of the parallel plates and the volume of the actuator is needed. In other work, a simplified geometric model is often used to develop this relationship. In contrast, we gather coupled position and pressure data while slowly compressing the actuator with the valve closed. From the several slow compression steps we fit a polynomial model to the measured displacement and volume relationship. We then compute the volume of the coupling from Boyle's law:

$$V_f(x) = \frac{P_o V_o}{P_f(x)}. \tag{8}$$

We repeat this experiment over several different initial pressures. Our computed change in volume with displacement, along with a quadratic fit for the relationship is shown in Fig. 4. We note that for the relationship in (8) the value of V_0 (the initial volume of the fabric coupling), uniformly scales the data and does not effect the goodness of fit. We select V_0 to best fit the force data obtained over the same compression steps, and find that the fabric pouch has an initial volume of 40 cm^3. As this data is obtained from several trials with different initial pressures, this result also validates the assumption that the volume of the coupling depends only on the position of the parallel plates and not on the internal pressure.

We now seek to observe the change in stiffness as the valve is opened and closed. In Fig. 5 we plot the change in pressure and force for both an open and closed valve while using both a 25g C02 cartridge ($V_a = 33\text{cm}^3$), and a larger pressure vessel ($V_a = 1900\text{cm}^3$), along with the predictions for pressure and force from the relationships in (2) and (3). We note in all cases good agreement between the theoretical models and the results. Another interesting effect is noted in observing the case of the large capacitor with the valve open. While the pressure does not change perceptibly (top), the contact force (bottom) does increase due to the increasing contact area, or increasing value of the $\frac{dV}{dx}$ term in (3).

C. Experimental Dynamic Impedance

To determine how impedance changes dynamically we generate a plot showing how maximum pressure changes with frequency of motion. We compress the coupling but moving the acrylic places in three sinusoidal cycles at constant frequency, and then record the peak pressure over the three cycles. To make the dynamic effects more apparent in our experiment we insert a 0.004" orifice into the pneumatic circuit between the valve and the capacitor. The resulting plot of maximum pressure as a function of frequency, averaged over two trials, is shown in Fig. 6. While the maximum pressure in the user coupling is approximately constant with frequency when the valve is closed, the maximum pressure increases slightly with frequency when the valve is open. This corresponds to the fluidic resistance between coupler and accumulator making a larger contribution to the perceived force by the user with high speed motion. In addition, we also compute the ratio of the maximum force when the valve is closed to maximum force when the valve is open, and find that this ratio decreases with frequency as the dynamic effects become more prominent.

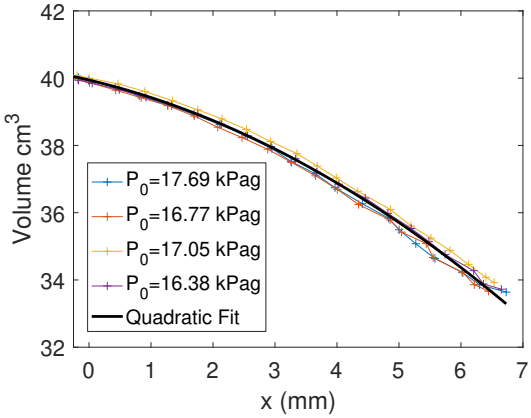

Fig. 4. The volume of the actuator with displacement of the parallel plates, and a quadratic fit for the data. This relationship is obtained from several trials and over several different initial pressures.

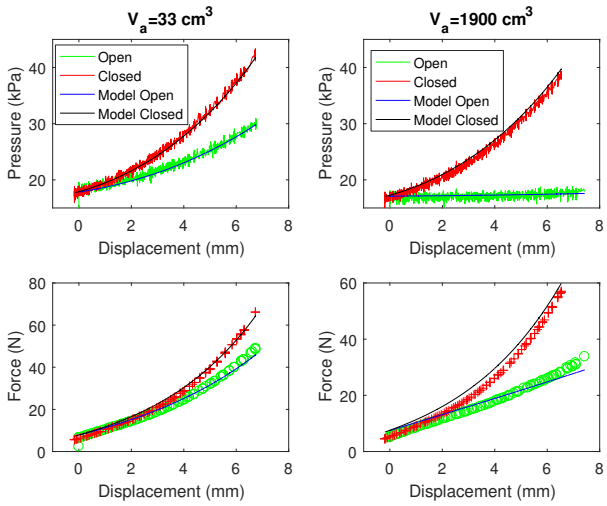

Fig. 5. Comparison of the pressure(top row) and force (bottom row). The left column is with a small capacitor, while the right column is with a large capacitor. Note that the model agrees well with the experimental data.

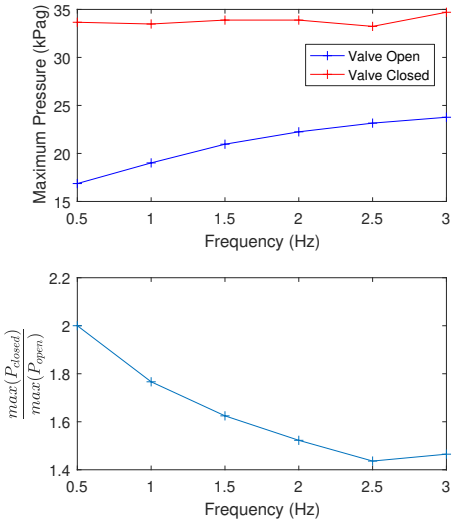

Fig. 6. (Top) The maximum pressure in the coupling when compressed in a sinusoidal pattern, and (bottom) the ratio of the maximum pressures when the valve is opened and closed. The maximum pressure appear independent of frequency when the valve is closed, but when the valve is open the peak pressure gradually increases as the resistance in the valve becomes more and more important in the dynamics. The ratio of maximum pressures (bottom) decreases over time.

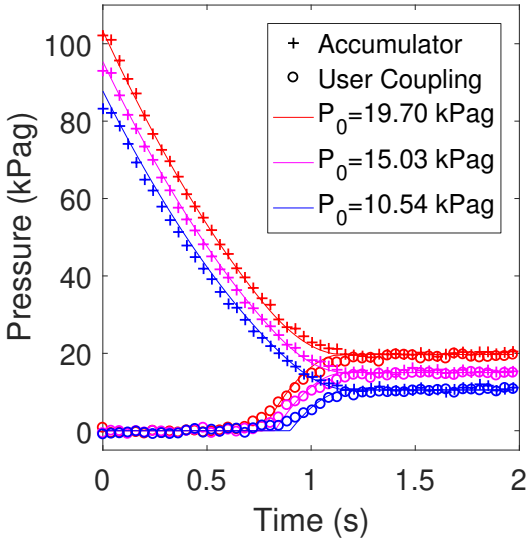

Fig. 7. The change in pressure in the accumulator and fabric user coupling at various initial pressures. Note that initially the pressure in the accumulator drops while the pressure in the fabric pouch remains at 0. Once the fabric pouch expands to its maximum volume, the pressure in the coupling builds until equilibrium. The solid lines are the model predictions and the points are experimental data.

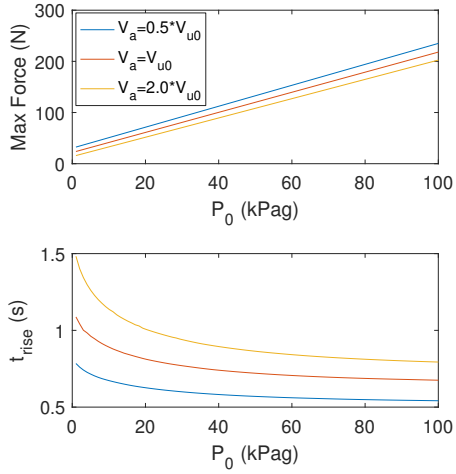

Fig. 8. The change in maximum force on the user with the valve open and response time with accumulator size and the initial circuit pressure. Maximum force increases with pressure and decreases with accumulator size, while the rise time displays opposite trends.

D. Refill Time

We experimentally examine the passive refill time of the device to get a sense of the device's bandwidth. We performed these tests by flattening the fabric actuator by hand (ensuring that it had approximately 0 initial volume), and then pressurizing the accumulator to a predefined pressure. We then opened the valve between the accumulator and coupling while recording the pressure of both at both locations. The 0.004" orifice remained in the circuit for this experiment. Our accumulator in this experiment is the 25g CO_2 cartridge with a volume of 33.1 cm^3. Fig. 7 shows a time history of pressure in the coupling and accumulator over time, along with the predictions obtained by solving the ODE introduced in Sec. IV for several different initial pressures. A few interesting characteristics of the pressure response can be observed both in the experimental results and the model predictions. When the valve is initially opened, the pressure in the accumulator immediately begins to drop, but the pressure in the user coupling remains near 0 as it expands. After the fabric pouch is fully expanded, the pressure rises to its equilibrium value. This seems to support our previous assumption that the fabric actuator expands at near atmospheric pressure until it reaches its maximum size, at which point it behaves similarly to a rigid chamber. The fit between the model and experimental results is obtained by fitting the parameter $\frac{C}{A^2}$ found in (6), which captures the resistance contribution of the valve, orifice resistor, and tubing between the accumulator and coupling.

VI. Model Based Design

We now discuss how to use the models for quasistatic impedance and response time to facilitate device design. In the case of system design we assume that the design of the user coupling is determined by the application and that the resistance of the circuit is fixed by physical constraints, such as the size of the valve and length of the tubing. This leaves the accumulator size and the initial pressure of the circuit as the variable parameters. To evaluate different designs we choose as our metrics the maximum force felt during free space motion (motion when the valve is open), and the response time. We assume the user coupling is the fabric pouch presented previously, and define the maximum force as the largest force felt over 8 mm of displacement computed using (3). We define the rise time as the time it takes an empty coupling to reach 62.3% of the equilibrium pressure, which we compute numerically by solving the (6) in conjunction with the mass pressure relationship for the

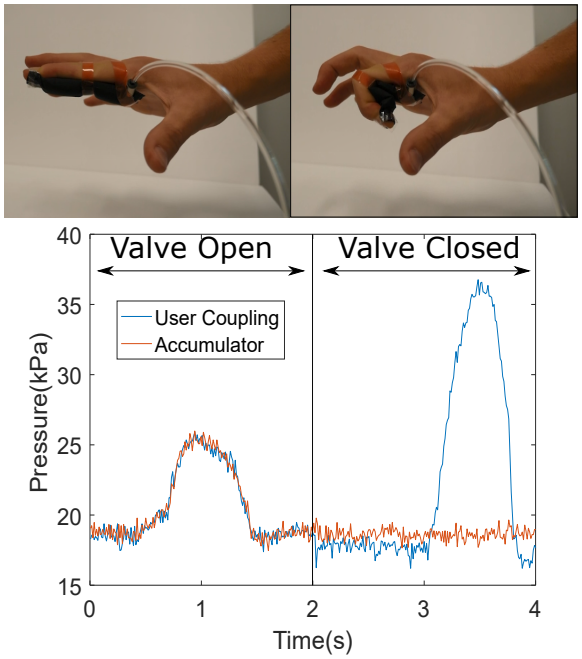

Fig. 9. An example application where a cylindrical bladder that is attached to a finger that is repeatedly flexed and extended. The valve changes from open to closed at 2 seconds. When the valve is open, the pressures in the coupling and the accumulator rise together. When the valve is closed, only the pressure of the coupling rises, and it rises to a much higher pressure level than when the valve was open.

coupling given in (7). The effect of accumulator size and the initial circuit pressure are shown in Fig. 8. Increasing internal pressure decreases rise time but increases the freespace force, while increasing the capacitor size decreases the maximum freespace force but increases rise time. Given a certain design criteria, these models could be used to choose the initial pressure and accumulator size to give specified performance.

VII. Sample Applications

To demonstrate possible applications on this device we present two sample applications. In one application a device provides resistance to the finger bending, and in another, an actuator worn at the finger tip is used to provide feedback in a button pressing task. These devices demonstrate two use scenarios: changing resistance to joint motion and changing interaction with the environment.

A. Finger Bending Device

To modulate resistance to finger bending, a cylindrical bladder made of TPU backed nylon is attached to the inside of a user's index finger with tape. When the user bends their finger inwards, the volume in the actuator decreases. The flexed and unflexed positions of the finger and the measured pressures in the coupling and accumulator are shown in Fig. 9. Before the valve is closed, the pressure in the coupling and accumulator are approximately equal, while after the valve is closed, the same motion of the finger leads to a much higher maximum pressure in the coupling, but no change in the accumulator pressure. The accumulator in this experiment is the 25g $C0_2$ cartridge.

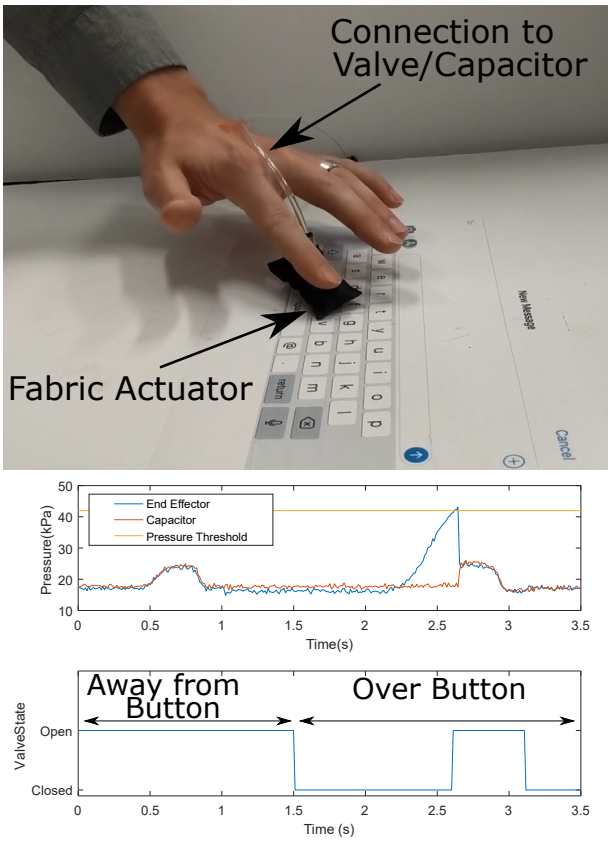

Fig. 10. A fabric coupling is attached to a finger and used as a button press device. The valve is open when the fingers are not pressing a button. When the device is over a button, the valve remains closed, giving the button a stiffer feel. If the button is pressed until the pressure passes a threshold, the valve opens, giving a snap-through effect.

B. Button Press Device

As a second example application, we present a small bubble worn on the finger that can give a button-like force response when grounded against any surface. A similar device could potentially allow any surface to have buttons layered on top of it in either augmented or virtual reality.

The button press system is shown in Fig. 10, and consists of a small fabric actuator taped to the finger. We achieve the button press sensation by actively opening or closing the valve based on the position of the user's finger and the pressure sensed in the end effector. When the user presses on a part of the surface that is not an active button, the valve remains open, meaning that the user feels relatively low resistance to the press. When the user begins to press on a part of the surface that is designated as a button, the valve closes and the user feels higher resistance. When the user presses hard enough that the pressure passes a threshold, the valve is opened and the user feels a snap-through effect, indicating that the button has been pressed. An example of the resulting pressures over a press on the table and a pressure on the virtual button is shown in Fig. 10. This is an example of the ability to change stiffness in a binary way to generate interesting effects.

In the response time results presented in Fig. 7 we inserted

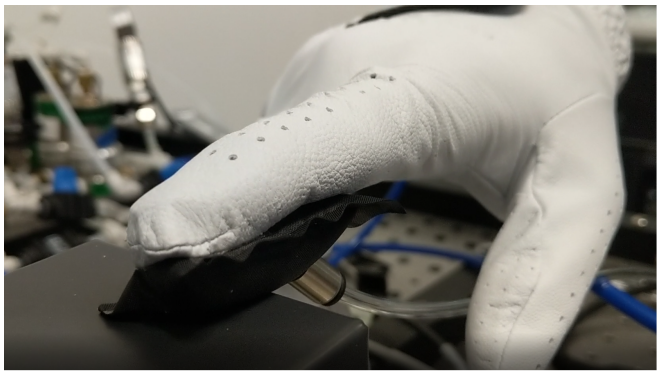

Fig. 11. A TPU pouch attached to a glove allows for a button-press haptic effect to be rendered. A video of this system is available in the supplementary material.

a 0.004" orifice into the fluidic circuit to make the dynamic characteristics of the circuit easier to measure. For the finger bending and button press demonstrations we have removed the orifice from the circuit, leading to a bandwidth that is significantly higher than measured previously. When the valve is open, there appears to be little lag between between the pressure in the accumulator and user coupling as shown in Fig. 9 and Fig. 10. In practice, the achievable bandwidth is primarily determined by the resistance to flow through the pneumatic circuit. As another practical consideration minor leakage in the system requires that we occasionally repressurize the system between experiments. In the future improved manufacturing could reduce this leakage, or another method could be used to occasionally restore pressure to the system.

VIII. Conclusion and Future Work

We have presented a closed circuit pneumatic device that is capable of providing compelling haptic sensations to the user without the need for a pressure source. We have presented models of the device's performance in terms of its quasistatic impedance and bandwidth, and used the models to inform device design. We also present experimental results on the dynamic impedance of the actuator, which we will model in future work.

Future work will include providing other ways to shape the force profile that the user feels during a motion. This may include multiplexing between different accumulators to be able to tune the value of quasistatic impedance. Instead of a binary valve connecting the user coupling and the accumulator, a proportional valve could be used that could provide a controllable dynamic damping effect. We are also interested in further developing the button pressing application. We will work on integrating an actuator onto each fingertip of a haptic glove, shown conceptually in Fig. 11. It seems plausible that this could create a compelling haptic typing glove that would allow a user to turn any surface into an array of buttons or a virtual keyboard that gives physical feedback when buttons are pressed.

References

[1] M. Philen, "Force tracking control of fluidic flexible matrix composite variable stiffness structures," *Journal of Intelligent Material Systems and Structures*, vol. 22, no. 1, pp. 31–43, 2011.

[2] S. I. Rich, R. J. Wood, and C. Majidi, "Untethered soft robotics," *Nature Electronics*, vol. 1, no. 2, p. 102, 2018.

[3] M. Wehner, R. L. Truby, D. J. Fitzgerald, B. Mosadegh, G. M. Whitesides, J. A. Lewis, and R. J. Wood, "An integrated design and fabrication strategy for entirely soft, autonomous robots," *Nature*, vol. 536, no. 7617, p. 451, 2016.

[4] M. T. Tolley, R. F. Shepherd, B. Mosadegh, K. C. Galloway, M. Wehner, M. Karpelson, R. J. Wood, and G. M. Whitesides, "A resilient, untethered soft robot," *Soft robotics*, vol. 1, no. 3, pp. 213–223, 2014.

[5] M. T. Tolley, R. F. Shepherd, M. Karpelson, N. W. Bartlett, K. C. Galloway, M. Wehner, R. Nunes, G. M. Whitesides, and R. J. Wood, "An untethered jumping soft robot," in *Intelligent Robots and Systems (IROS 2014), 2014 IEEE/RSJ International Conference on*. IEEE, 2014, pp. 561–566.

[6] S. Follmer, D. Leithinger, A. Olwal, N. Cheng, and H. Ishii, "Jamming user interfaces: programmable particle stiffness and sensing for malleable and shape-changing devices," in *Proceedings of the 25th annual ACM symposium on User interface software and technology*. ACM, 2012, pp. 519–528.

[7] A. A. Stanley, J. C. Gwilliam, and A. M. Okamura, "Haptic jamming: A deformable geometry, variable stiffness tactile display using pneumatics and particle jamming," in *World Haptics Conference (WHC), 2013*. IEEE, 2013, pp. 25–30.

[8] T. M. Simon, R. T. Smith, and B. H. Thomas, "Wearable jamming mitten for virtual environment haptics," in *Proceedings of the 2014 ACM International Symposium on Wearable Computers*. ACM, 2014, pp. 67–70.

[9] I. Zubrycki and G. Granosik, "Novel haptic glove-based interface using jamming principle," in *Robot Motion and Control (RoMoCo), 2015 10th International Workshop on*. IEEE, 2015, pp. 46–51.

[10] I. Choi, E. W. Hawkes, D. L. Christensen, C. J. Ploch, and S. Follmer, "Wolverine: A wearable haptic interface for grasping in virtual reality," in *Intelligent Robots and Systems (IROS), 2016 IEEE/RSJ International Conference on*. IEEE, 2016, pp. 986–993.

[11] D. C. Rennels and H. M. Hudson, *Pipe Flow: A Practical and Comprehensive Guide*. John Wiley & Sons, 2012.